High-Permittivity Rectangular Dielectric Rod Waveguides for 110-325 GHz

J. P. Pousi, D. V. Lioubtchenko, and A. V. Räisänen

Aalto University School of Electrical Engineering, Department of Radio Science and Engineering,
SMARAD Centre of Excellence
PO Box 13000, FI-00076 Aalto, Finland

***Abstract*-Dielectric rod waveguides made of silicon and sapphire are characterized with simulations and measurements for 110-325 GHz in this paper. Such waveguides provide a good basis for many kinds of active and passive components at mm-wavelengths.**

I. Introduction

Dielectric rod waveguides are an interesting alternative for the base of many components in millimetre-wave and terahertz frequencies. Dielectric waveguides offer lower losses than metal waveguides and good possibilities for component integration on the waveguide surface.

Earlier several components have been designed based on dielectric rod waveguides like antennas, flexible waveguides, couplers and power dividers. Active components include amplifiers and tunable phase shifter [1]-[6].

Dielectrics with different values of permittivity can be used, but often low-permittivity materials require more complex feeding structures. In this paper relatively high-permittivity dielectric rod waveguides made of silicon (ε_r=11.9, $tan\ \delta \approx 10^{-4}\ldots10^{3}$) and sapphire ($\varepsilon_{r\parallel}$=11.56, $\varepsilon_{r\perp}$=9.39, $tan\ \delta \approx 10^{-4}$) are characterized with simulations and measurements for 110-170 GHz and 220-325 GHz.

II. Dielectric rod waveguides

Many different kinds of dielectric waveguides can be used at millimetre wavelengths. Main types of rectangular dielectric waveguiding structures are a dielectric rod waveguide and an image waveguide. Image waveguide can also include an insulating layer. This paper concentrates on open dielectric rod waveguides that are fed with a regular metal waveguide.

The cross-section size of the dielectric rod is an important parameter that affects greatly on the waveguiding properties. Choosing a rectangular cross-section other than a square decreases the possibilities for cross-polarization. Design rule a/b = 0.5, where a is the horizontal length and b the vertical length has been earlier successfully used for high-permittivity dielectrics at W band. Cross-section can be chosen according to the desired central frequency with the formula k_0b = 1.7…1.9, where $k_0 = 2\pi/\lambda_0$. λ_0 is the wavelength of the centre frequency [7].

From these conditions, different DRW cross-sections sizes are calculated in Table I.

TABLE I
DRW CROSS-SECTION FOR DIFFERENT FREQUENCIES

Metal waveguide	Centre frequency (GHz)	*a* (mm)	*b* (mm)
WR-6	140	0.29-0.32	0.58-0.65
WR-5	180	0.23-0.25	0.45-0.50
WR-4	220	0.18-0.21	0.37-0.41
WR-3	270	0.15-0.17	0.30-0.34

For a good matching with the metal waveguide DRW requires a taper section. Several types of tapers can be imagined, e.g., horizontal, vertical, pyramidal or dovetail tapers. However, as the rod dimensions get small often the most practical solution in manufacturing point of view is the vertical taper. For this reason, the waveguides studied in this paper include all vertical tapers.

III. Simulations and measurements

A standard rectangular metal waveguides (WR-6, cross-sectional area of 1.65 x 0.83 mm^2, WR-3, 0.86 x 0.43 mm^2) is used as a feed element. In the simplest design the dielectric rod is inserted in the middle of the waveguide opening. It is difficult to fix the rod exactly in the middle of the metal waveguide; one possible solution is to use thin porous Teflon films around the rod to fit it between the walls of the metal waveguide. However, this is not a very durable solution for real applications, but it can be used in demonstration prototypes.

Ansoft HFSS^{TM} software based on the Finite element method (FEM) is used to simulate and study DRW antenna structures. Different simulations are performed to obtain a better comprehension of dielectric rod waveguides and antennas. Fig. 1 presents the basic simulation setup (quarter of the structure is needed). A transition from a standard rectangular waveguide to another one through a sapphire rod

is simulated with different cross-section dimensions and tapers to find the optimal structure. It is important to note that in HFSS the air box and its radiation boundary should be set far enough from the rod. Recommendation in HFSS is that the radiation boundary should be set at least $\lambda/4$ away from any radiating source, otherwise the results will be distorted. It has to be also noticed that this simulation setup does not take into account the currents on the metal waveguide external surfaces. These currents would probably cause extra radiation to the system.

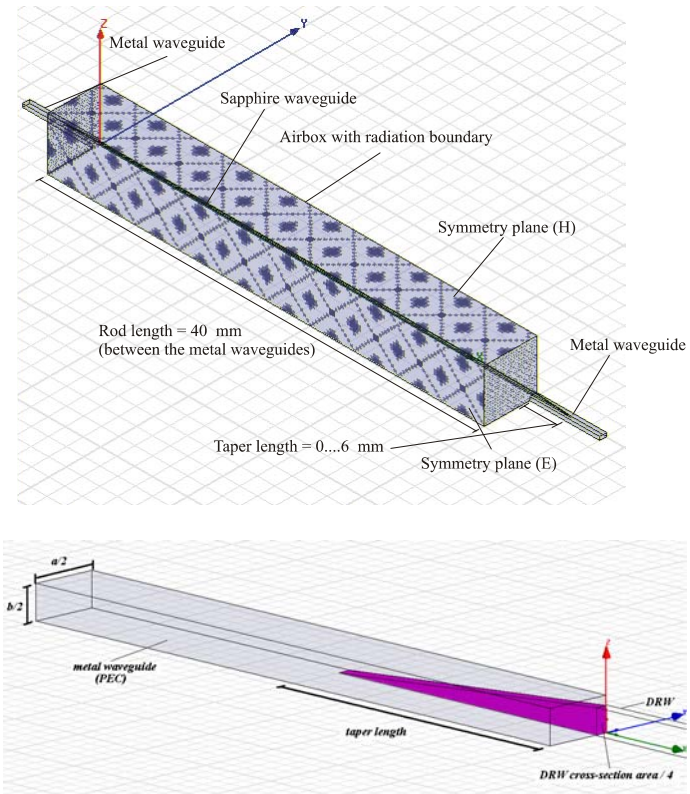

Figure 1. Basic simulation setup for metal waveguide – DRW simulations.

A. Simulation results for 110-170 GHz: taper length

First different taper lengths are studied with an anisotropic sapphire rod with 0.30 x 0.60 mm^2 cross-section. Simulations are performed with the taper length from 0 to 6 mm. Anisotropy in this case means that the permittivity of the material depends on the axis. For monocrystalline sapphire in the longitudinal axis (x-axis in the simulation) $\varepsilon_r = 11.56$ and for other axis $\varepsilon_r = 9.39$ (y- and z-axis). Both ends of the rod have the same taper length. The rod length between the metal waveguides is 40 mm. The simulated transmission and reflection coefficients are presented in Figs. 2 and 3.

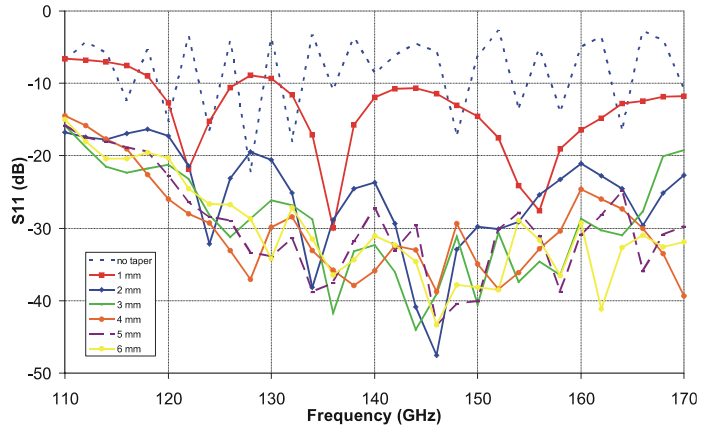

Figure 2. Simulated S_{11} of a sapphire rod waveguide with different taper length.

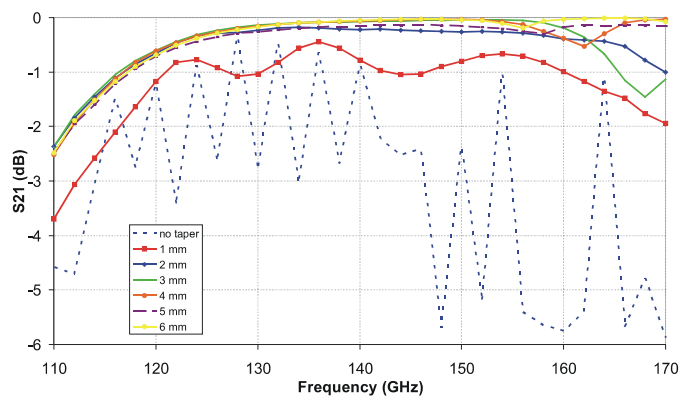

Figure 3. Simulated S_{21} of a sapphire rod waveguide with different taper length.

As expected, the benefit of the taper section is clearly seen in both figures when using longer taper section. However, only a slight improvement is seen for tapers longer than 3 mm. The benefit of the longer tapers seems to be the shallower dips in the higher frequency end in S_{21}. A 6-mm taper has already an almost flat S_{21} in the higher frequency range. It can be also seen that in lower frequencies the matching is not very good and even a longer taper does not improve it. One reason might be that the cross-section area of the rod is not optimal for the whole frequency range. Fig. 4 presents the simulated E field in sapphire rod waveguide transition between two metal waveguides at 140 GHz. Taper length in this case is 3 mm. Field propagating partially outside the sapphire rod can be observed.

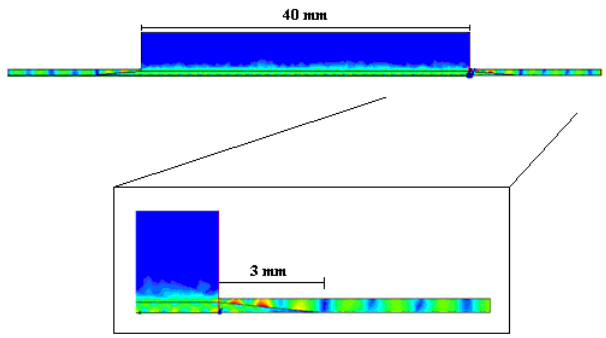

Figure 4. Simulated E field in the sapphire rod waveguide transition (quarter in the setup) between two metal waveguides at 140 GHz.

B. Simulation results for 110-170 GHz: DRW cross-section

In the next stage, propagation characteristics with different cross-section sizes are studied. As calculated earlier the optimum cross-section dimensions are b = 0.58-0.65 mm and a = 0.29-0.32 mm. As the metal waveguide dimensions are 1.65 x 0.83 mm^2, b can not be larger than 0.83 mm. The cross-section size in the simulation is varied from 0.50 x 0.25 mm^2 to 0.82 x 0.41 mm^2. The rod length between the metal waveguides also in this simulation setup is 40 mm. The feed taper is 3 mm in both ends. Simulated reflection and transmission coefficients are presented in Figs. 5 and 6.

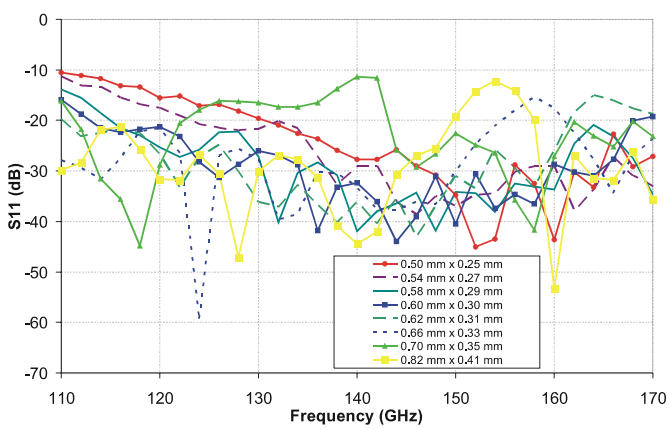

Figure 5. Simulated S_{11} of a sapphire rod waveguide with different taper length.

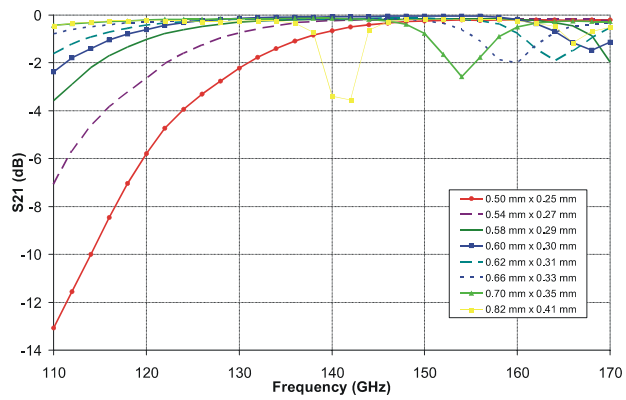

Figure 6. Simulated S_{21} of a sapphire rod waveguide with different taper length.

According to the simulation results it is clear that the matching is improved at lower frequencies when the cross-section area is larger. On the other hand, matching becomes unstable at higher frequencies as the cross-section area is increased. Dips can be seen in S_{21}. As the height of the rod is increased almost to equal to the height of the metal waveguide the dip becomes deeper and it is also shifted to a lower frequency. Such dips are due to the increased radiation from the feed because of the phase mismatch between the wave inside the taper and the wave in the metal waveguide [8]. Longer tapers would make the dips smaller as it is found out in the taper length simulations. The cross-section of 0.60 x 0.30 mm^2 seems to offer a good compromise with the overall matching over a wide frequency range with a relatively low mismatch at the higher frequency end.

C. Measurement results for 110-170 GHz

The measurements are done with Elmika scalar network analyzer, R2402E. Small pieces of porous Teflon sheets are used to hold and position DRWs in the center of the metal waveguides.

Four different DRWs are measured:

- Silicon short: 40 mm (32 mm + 2x4 mm tapers), 0.31 x 0.61 mm^2 cross-section
- Silicon long: 58 mm (50 mm + 2x4 mm tapers), 0.31 x 0.62 mm^2 cross-section
- Sapphire short: 18 mm (10 mm + 2x4 mm tapers), 0.30 x 0.60 mm^2 cross-section
- Sapphire long: 58 mm (50 mm + 2x4 mm tapers), 0.30 x 0.60 mm^2 cross-section

Measurement results are presented in Figs. 7 and 8. The black line in Fig. 7 is the measured transmission coefficient for two WR-6 metal waveguides that are connected together.

The black line in Fig. 8 is the S_{11} of an open-ended WR-6 waveguide.

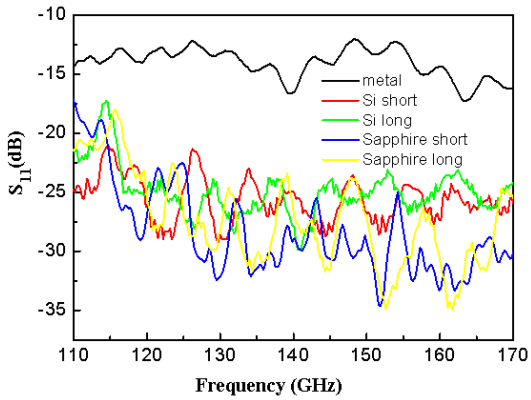

Figure 7. Measured S_{11} in D band.

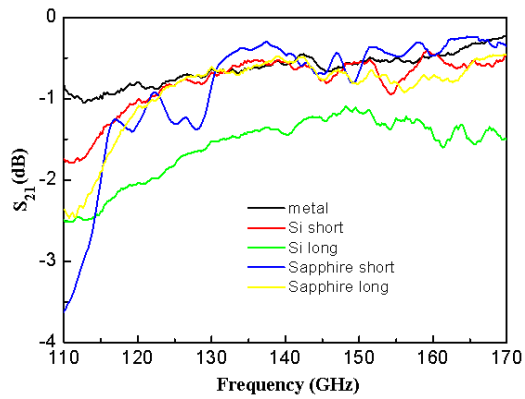

Figure 8. Measured S_{21} in D band.

The insertion loss is about 1 dB higher for the long silicon rod waveguide over the whole frequency range. In sapphire the difference is not so clear. This result is expected due to higher loss tangent of silicon. The return loss of an open-ended WR-6 is about 10 dB higher than with any of the DRWs.

D. Simulation results for 220-325 GHz: DRW cross-section

The dimensions of the rod are defined in similar way as in the case of the D-band antenna. The cross-section dimensions at 310 GHz central frequency are $b \approx$ 0.26-0.30 mm and $a \approx$ 0.13-0.15 mm. As the metal waveguide dimensions are very small (0.86 x 0.43 mm^2) the accuracy and rod pointing problems are also emphasized in this frequency range.

The total rod length is chosen to be 12 mm including a 2-mm taper section in both ends. Fig. 9 and Fig. 10 present the simulated S_{11} and S_{21} of the sapphire rod waveguide with different cross-sections.

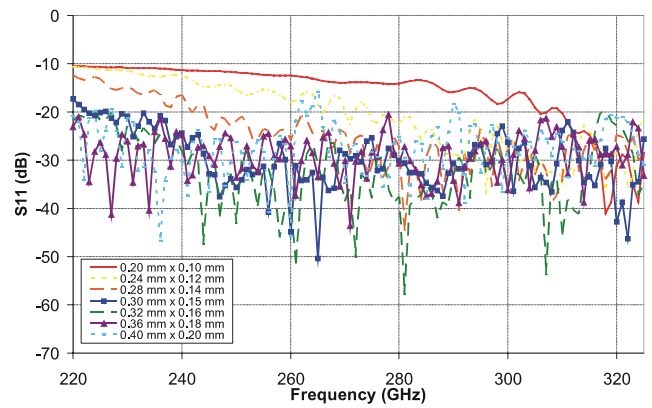

Figure 9. Simulated S_{11} of a sapphire rod waveguide with different cross-section.

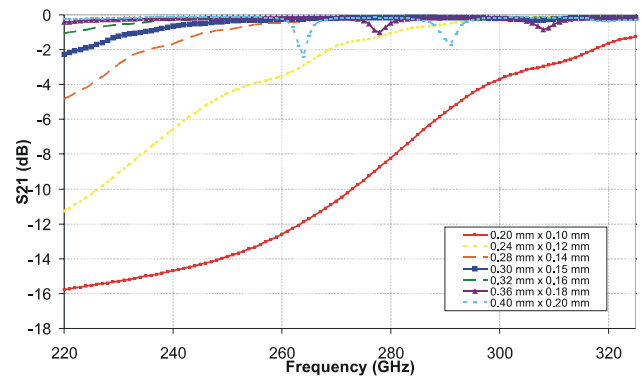

Figure 10. Simulated S_{21} of a sapphire rod waveguide with different cross-section.

According to the simulation results, the reflections are significantly larger in rods having the cross-section area smaller than 0.30 x 0.15 mm^2. With larger cross-sections similar dips that have been observed in D band occur, but they are significantly smaller. Cross-section area of 0.15 x 0.30 mm^2 seems to be a good choice for this frequency range. It also leaves some margin for manufacturing tolerances as the performance remains quite stable in little larger or smaller dimensions.

E. Simulation results for 220-325 GHz: taper length

Figs. 11-13 present the simulated results of the sapphire rod waveguide with the cross-section of 0.30 x 0.15 mm^2 with different taper lengths. According to the simulated S parameters tapers longer than 2 mm do not improve the performance significantly. That is clearly visible in both S_{11} and S_{21}.

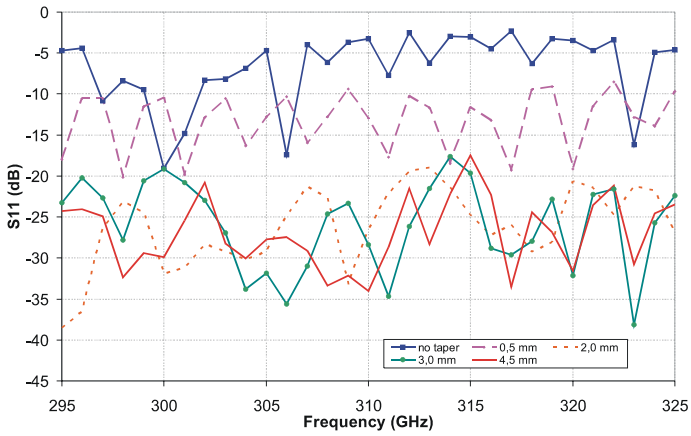

Figure 11. Simulated S_{11} of a sapphire rod waveguide with different taper length.

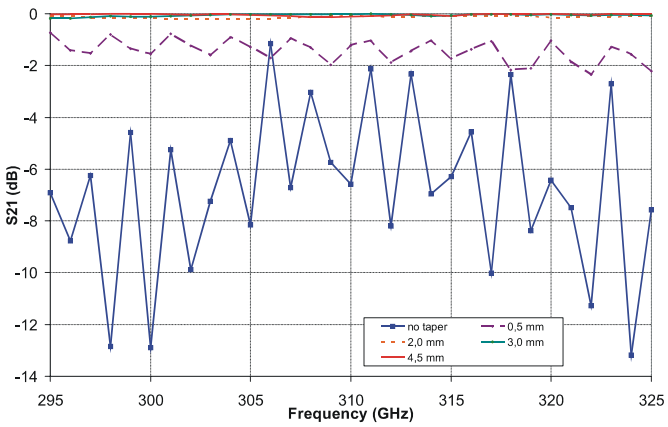

Figure 12. Simulated S_{21} of a sapphire rod waveguide with different taper length.

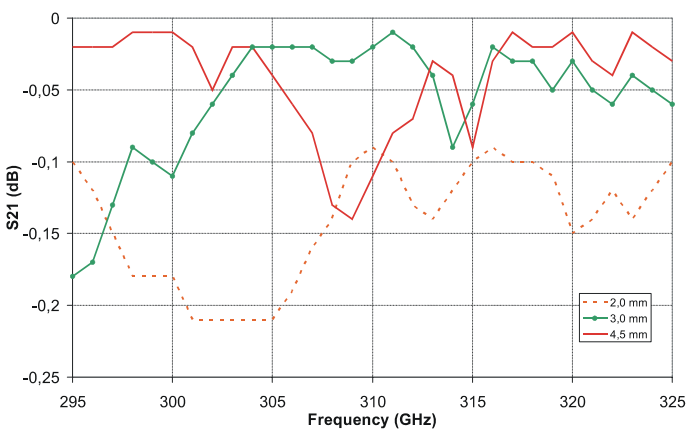

Figure 13. Simulated S_{21} of a sapphire rod waveguide with different taper length (2.0-4.5 mm).

F. Measurement results for 220-325 GHz

The measurements are done with Agilent N5260A vector network analyzer. Fig. 14 presents a photograph of the measurement setup. Special WR-3 waveguides are used to facilitate the matching of the DRW. The DRW is made of silicon and its length is 12 mm including 2 mm taper section in both ends. The cross-section area is 0.30 x 0.15 mm^2.

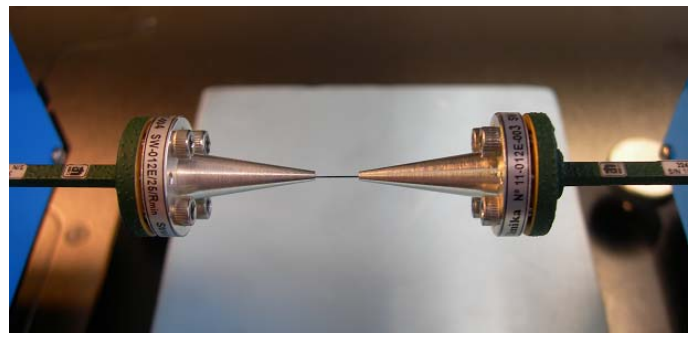

Figure 14. A photograph of the measurement setup.

Figs. 15 and 16 present the measured S_{11} and S_{21} compared with the simulations. Especially in S_{21} the difference between the measurements and simulations is rather large. As the frequency increases the matching of the DRW becomes more and more difficult. In this case a porous Teflon film is used for positioning of the DRW and its effect is larger than in the D band. Also the manufacturing tolerances become more critical. However, at high frequencies relatively low transmission loss is achieved, less than 3 dB.

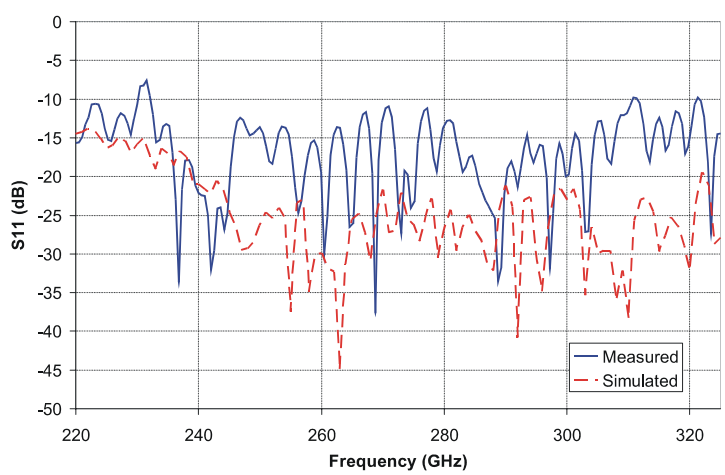

Figure 15. Measured and simulated S_{11} of the silicon rod waveguide.

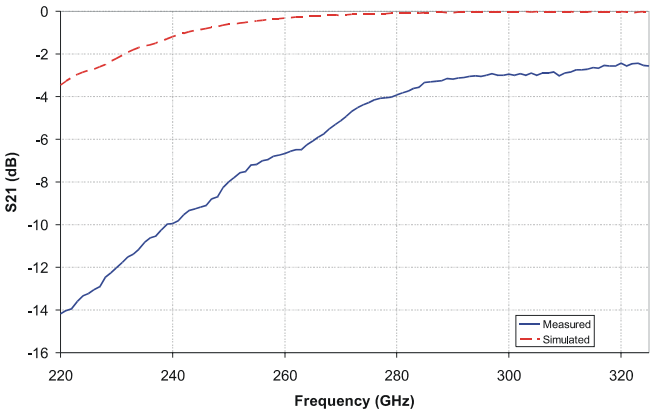

Figure 16. Measured and simulated S_{21} of the silicon rod waveguide.

IV. Conclusions

In this paper, DRWs have been studied with simulations and measurements for 110-325 GHz. In simulations the DRW performance is analysed with different cross-section sizes and taper lengths. D-band measurements of the manufactured prototype show that very good agreement with simulations can be achieved. At higher frequency band, 220-325 GHz, the prototype manufacturing tolerances and matching are more demanding, and in order to meet the simulated results more sophisticated methods are required than those available at this stage.

However, it has been shown that the dielectric rod waveguides are a potential alternative for the base of many active and passive components also at sub-millimetre wavelengths. Measurements at higher frequency band have been made only with a silicon prototype. However, silicon becomes rather fragile to process for a rod waveguide at this frequency range. Sapphire would offer a better durability.

Acknowledgment

This work is supported by the Finnish Academy of Science. Processing work for the prototypes has been partly done at MC2 Nanofabrication Laboratory, Chalmers University of Technology, Gothenburg, Sweden. It has been financed by the FP6-Research Infrastructures program MC2ACCESS through Contract No: 026029.

D-band measurements have been partly done at the facility of Elmika Co. in Vilnius, Lithuania.

References

[1] A. Hofmann, E. Horster, J. Weinzierl, L.-P. Schmidt, and H. Brand, “Flexible low-loss dielectric waveguides for THz frequencies with transitions to metal waveguides,” in *Proc. of the 33rd European Microwave Conf.*, Munich, Germany, October 2003, pp. 955-958

[2] S.M. Hanham, T.S. Bird, B.F. Johnston, A.D. Hellicar, and R.A. Minasian, ”A 600 GHz dielectric rod antenna,” in *Proc. of the 3rdEuropean Conference of Antennas and Propagation (EuCAP 2009)*, Berlin, Germany, March 2009, pp. 1645-1647.

[3] J. Weinzierl, J. Richter, G. Rehm, and H. Brand, ”Simulation and measurement of dielectric antennas at 150 GHz,” in *Proc. of the 29th Eur. Microwave Conf.*, Munich, Germany, 1999, pp. 185-188.

[4] J.P. Pousi, S.N. Dudorov, D.V. Lioubtchenko, and A.V. Räisänen, ”Frequency selective coupler for W band based on power transfer in dielectric rod waveguides,” in *Proc. of the 4thEuropean Conference of Antennas and Propagation (EuCAP10)*, Barcelona, Spain, 11-16 April, 2010, paper 1840244.

[5] J.P. Pousi, D. Lioubtchenko, S. Dudorov, and A.V. Räisänen, ”Dielectric rod waveguide travelling-wave amplifier based on AlGaAs/GaAs heterostructure,” in *Proc. of the 38thEuropean Microwave Conference*, Amsterdam, Netherlands, 28-31 October, 2008, pp. 1082-1085.

[6] D.V. Lioubtchenko, P. Pousi, S.N. Dudorov, and A.V. Räisänen, ”Millimetre-wave phase shifter based on dielectric rod waveguide,” in *Proc. of the 38thEuropean Microwave Conference*, Amsterdam, Netherlands, 28-31 October, 2008, pp. 1204-1206.

[7] D.V. Lioubtchenko, S.N. Dudorov, J.A. Mallat, and A.V. Räisänen, ”Dielectric rod waveguide antenna for W band with good input match,” *IEEE Microwave and Wireless Components Letters,* vol. 15, no. 1, pp. 4-6, Jan. 2005.

[8] S. Dudorov, *Rectangular Dielectric Waveguide and Its Optimal Transition to a Metal Waveguide*, Doctoral Thesis, Helsinki University of Technology, Radio Laboratory, Otamedia 2002.